

# Clustering and Correlations in Neutron Haloes

Nigel ORR<sup>\*)</sup>

*LPC-ISMRA, Bd Maréchal Juin, 14050 Caen Cedex, France*

(Received November 1, 2018)

In the present paper clustering and correlations within halo systems is explored. In particular, the application of neutron-neutron interferometry and Dalitz-plot type analyses is presented through the example provided by the dissociation of  $^{14}\text{Be}$ . A novel approach for producing and detecting bound neutron clusters is also described. The observation of some 6 events with characteristics consistent with the liberation of a multineutron cluster in the breakup of  $^{14}\text{Be}$  – possibly in the channel  $^{10}\text{Be} + ^4\text{n}$  – is discussed.

## §1. Introduction

Clustering, which has long been known to occur along the line of beta stability, also appears in more exotic forms as the drip-lines are approached. For example,  $2\alpha - Xn$  molecular-like configurations have been observed in excited states of  $^{10,12}\text{Be}$ <sup>1)</sup>. The most spatially extreme form of clustering are the neutron haloes which occur as the ground states of some nuclei at the limits of particle stability. Perhaps the most intriguing of the halo systems are the Borromean two-neutron halo nuclei ( $^6\text{He}$ ,  $^{11}\text{Li}$  and  $^{14}\text{Be}$ ), in which the two-body subsystems (core- $n$  and  $n - n$ ) are unbound. Such behaviour naturally gives rise to the question of the correlations between the constituents. Even in the case of the most studied of these nuclei,  $^6\text{He}$  and  $^{11}\text{Li}$ , little is known in this respect. In the first part of this paper we explore the nature of these correlations through the application of interferometry and Dalitz-plot type analyses to kinematically complete measurements of dissociation.

On a more speculative note, the production and detection of bound multineutron clusters in the breakup of very neutron-rich secondary beams is explored in the final section of this paper. This approach exploits the possibility that multineutron halo nuclei and other very neutron-rich systems contain components of the wavefunction in which the neutrons exist in a relatively compact cluster-like configuration. A new method is introduced here for the direct detection of neutral clusters and the results obtained from an analysis of data acquired with beams of  $^{11}\text{Li}$  and  $^{14}\text{Be}$  is presented.

## §2. Experimental Setup

The results described here were derived from data taken using what is now a relatively standard experimental configuration for kinematically complete measurements of the breakup of neutron-rich beams<sup>3)</sup>. The secondary beams ( $\overline{E}$ =30-50 MeV/nucleon) were prepared from a 63 MeV/nucleon  $^{18}\text{O}$  primary beam using the LISE3 spectrometer at GANIL. The beam particles were tracked onto the breakup

---

<sup>\*)</sup> e-mail: orr@caelav.in2p3.fr

targets (C and Pb) using two position sensitive parallel plate avalanche counters. The charged fragments from dissociation were identified using a large area position sensitive Si-CsI telescope centred at zero degrees and located  $\sim 15$  cm downstream of the target.

The neutrons emitted at forward angles were detected using the 99 elements of the DEMON array. The array covered angles between  $+13^\circ$  and  $-40^\circ$  in the horizontal plane and  $\pm 14^\circ$  in the vertical with the modules arranged in a staggered configuration at distances between 2.5 and 6.5 m from the target<sup>2)</sup>. Such a geometry provided for a relatively high two-neutron detection efficiency (1.5%) whilst reducing the rate of cross-talk — both intrinsically and via the use of an off-line rejection algorithm — to negligible levels<sup>2), 3)</sup>.

### §3. Correlations in Two-Neutron Halo Nuclei

We have explored the spatial configuration of the halo neutrons at breakup through the application of the technique of intensity interferometry — an approach first developed for stellar interferometry by Hanbury-Brown and Twiss in Australia in the 1950's and 60's<sup>6)</sup> and later extended to source size measurements in high energy collisions<sup>7)</sup>. The principle behind the technique is as follows: when identical particles are emitted in close proximity in space-time, the wave function of relative motion is modified by the FSI and quantum statistical symmetries<sup>8)</sup> — in the case of halo neutrons the overwhelming effect is that of the FSI<sup>4)</sup>. Intensity interferometry relates this modification to the space-time separation of the particles at emission as a function of the four-momenta of the particles through the correlation function  $C_{nn}$ , which is defined as,

$$C_{nn}(p_1, p_2) = \frac{d^2n/dp_1 dp_2}{(dn/dp_1)(dn/dp_2)} \quad (3.1)$$

where the numerator is the measured two-particle distribution and the denominator the product of the independent single-particle distributions<sup>4)</sup>. As is generally the case, the single-particle distributions have been generated in our work via event mixing. Importantly, in the case of halo neutrons special consideration must be given to the strong residual correlations<sup>4)</sup>. Experimentally care needs to be taken to eliminate cross talk<sup>2)</sup>.

As a first step, the measurements of breakup on a Pb target of  ${}^6\text{He}$ ,  ${}^{11}\text{Li}$  and  ${}^{14}\text{Be}$  were analysed<sup>4)</sup>. The choice of a high-Z target was made to privilege Coulomb induced breakup, whereby the halo neutrons may in a first approximation act as spectators and for which simultaneous emission may be expected to occur. The correlation functions derived from the data, assuming simultaneous emission, were compared to an analytical formalism based on a Gaussian source<sup>9)</sup>. Neutron-neutron separations of  $r_{nn}^{RMS} = 5.9 \pm 1.2$  fm ( ${}^6\text{He}$ ),  $6.6 \pm 1.5$  fm ( ${}^{11}\text{Li}$ ) and  $5.6 \pm 1.0$  fm ( ${}^{14}\text{Be}$ ) were thus extracted. These results appear to preclude any strong dineutron component in the halo wavefunctions at breakup; a result which, for  ${}^6\text{He}$  is in line with a recent radiative capture experiment we have performed<sup>10)</sup>. It is interesting in this context to compare these results to the RMS neutron-proton separation of

3.8 fm in the deuteron (the only bound two nucleon system).

The same analysis has been applied to dissociation of  $^{14}\text{Be}$  by a C target, in order to investigate the influence of the reaction mechanism. A result which hints at a somewhat larger separation,  $r_{nn}^{rms} = 7.6 \pm 1.7$  fm, was obtained. This raises the question as to whether simultaneous emission can be assumed a priori. In principle, the analysis of the correlation function in two dimensions, transverse and parallel to the total momentum of the pair, would allow for the unfolding of the source size and lifetime<sup>9)</sup>. Such an analysis requires a much larger data set than presently available. The two-neutron halo, however, is far less complex than the systems usually studied via interferometry (for example, heavy-ion collisions<sup>8)</sup>). Moreover, the simple three-body nature of the system breaking up suggests that any delay in the emission of one of the neutrons will arise from core-n FSI/resonances in the exit channel, a process that may be expected to be enhanced for nuclear induced breakup.

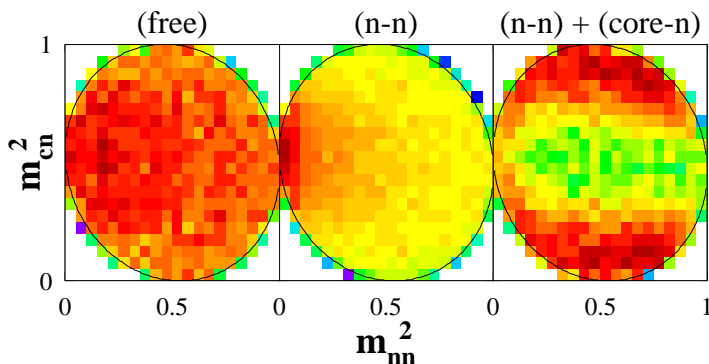


Fig. 1. Dalitz plot for the simulated decay of  $^{14}\text{Be}$  (see text). In the left panel no FSI are included.

Correlations in three-particle decays are commonly encountered in particle physics and are typically analysed using plots of the squared invariant masses of particle pairs ( $M_{ij}^2, M_{ik}^2$ ), with  $M_{ij}^2 = (p_i + p_j)^2$ ; a technique developed by the Australian physicist Richard Dalitz in the early 1950's<sup>11)</sup>. In Dalitz-plot representations, FSI or resonances lead to a non-uniform population of the surface within the kinematic boundary defined by energy-momentum conservation and the decay energy. In the present case, the core+n+n system exhibits a distribution of decay energies ( $E_d$ ). The  $E_d$  associated with each event will thus lead to a different kinematic boundary, and the resulting plot containing all events cannot be easily interpreted. We have thus introduced a normalised invariant mass,

$$m_{ij}^2 = \frac{M_{ij}^2 - (m_i + m_j)^2}{(m_i + m_j + E_d)^2 - (m_i + m_j)^2} \quad (3.2)$$

which ranges between 0 and 1 (that is, a relative energy  $E_{ij} = M_{ij} - m_i - m_j$  between 0 and  $E_d$ ) for all events and exhibits a single kinematic boundary. Examples of how n-n and core-n FSI may manifest themselves in the Dalitz plot for the decay of  $^{14}\text{Be}$  are illustrated in Fig. 1, whereby events have been simulated according to

the simple interacting phase-space model described in ref. <sup>5)</sup>. The inputs were an  $E_d$  distribution following that measured <sup>3)</sup>, the  $C_{nn}$  obtained with the C target, and a core-n resonances with  $\Gamma = 0.3$  MeV at  $E_0 = 0.8$  MeV. Note that due to the normalisation the (squared) core-neutron invariant mass does not present a simple structure directly related to the energy of the resonance/FSI <sup>5)</sup>.

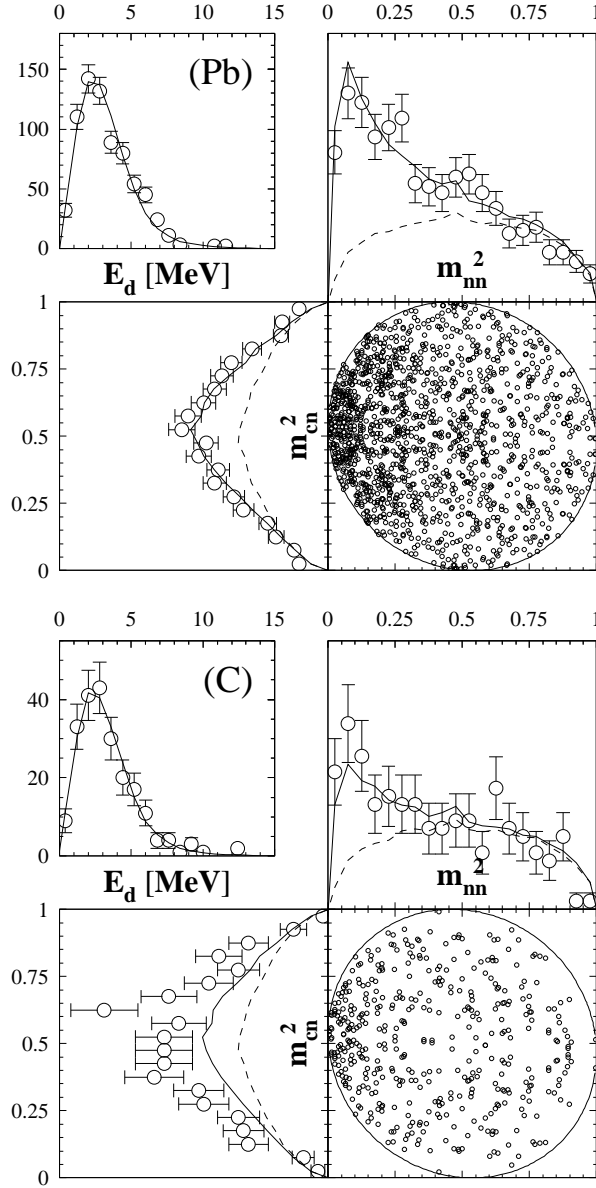


Fig. 2. Dalitz plot and the projections onto the squared invariant masses for the dissociation of  $^{14}\text{Be}$  by Pb (upper) and by C (lower panels). The lines are the phase-space model simulations with/without (solid/dashed) n-n FSI. The inset shows the measured  $E_d$  spectrum.

The Dalitz plot for the data from the dissociation by Pb (Fig. 2, upper panel)

presents a strong n-n FSI and a uniform density for  $m_{nn}^2 j \sim 0.5$ . Indeed, the n-n FSI alone describes very well the projections onto both axes, and therefore suggests that core-n resonances are not present to any significant extent. This result confirms the hypothesis of simultaneous n-n emission employed in the original analysis of the dissociation of  $^{14}\text{Be}$  by Pb<sup>4)</sup>. The  $r_{nn}^{RMS}$  so extracted,  $5.6 \pm 1.0$  fm, may thus be considered to represent the n-n separation in the halo of  $^{14}\text{Be}$ .

For dissociation by the C target (Fig. 2, lower panel), despite the lower statistics, two differences are evident. Firstly, the n-n signal is weaker, indicating that a significant delay has occurred between the emission of each neutron. Second, and more importantly, the agreement between the model including only the n-n FSI and the data for  $m_{cn}^2$  is rather poor. In order to verify whether this disagreement corresponds to the presence of core-n resonances the core-n relative energy,  $E_{cn}$ , has been explored. It has been reconstructed for the simulations incorporating only the n-n FSI and compared in Fig. 3 to the data (the model calculations have been normalized to the data above 4 MeV). For dissociation by Pb, the inclusion of only the n-n FSI provides a very good description of the data, with the exception of small deviations below 1 MeV. This is in line with the Dalitz-plot analysis discussed above.

The deviations observed for the C target between the measured  $m_{cn}^2$  and the simulation including only the n-n FSI clearly correspond to structures in the  $E_{cn}$  spectrum. Moreover, these structures are located at energies that are in line with those of states previously reported in  $^{13}\text{Be}$ : the supposed  $d_{5/2}$  resonance at 2.0 MeV<sup>12), 13)</sup> and a lower-lying state(s)<sup>14), 13), 15)</sup>. The model-to-data ratio is about 1/2, indicating that the peaks correspond to resonances formed by one of the neutrons in almost all decays; the solid line accounts for the contribution of the neutron not interacting with the core. If we add to the phase-space model with n-n FSI core-n resonances ( $\Gamma = 0.3$  MeV) at  $E_0 = 0.8, 2.0$ <sup>13)</sup> and 3.5 MeV<sup>\*</sup>) with intensities of 45, 35 and 20%, respectively, the data are well reproduced (dashed line). In the case of dissociation by Pb, the lowest-lying level(s) appears to be present in at most 10% of events.

In the context of the influence of the reaction mechanism, it is worthwhile noting that whilst some 35% of the two-neutron removal cross section on the Pb target is attributable to nuclear induced breakup<sup>3)</sup>, the requirement of two neutrons in coincidence with the  $^{12}\text{Be}$  core in the present analysis reduces this to some 15% – approximately half of the two-neutron removal cross section arises from absorption.

By combining the information extracted from the core-n channel with the n-n correlation functions, the analysis can be extended to extract the average lifetime of the core-n resonances. If the n-n separation in  $^{14}\text{Be}$  is fixed to that obtained for dissociation by Pb,  $r_{nn}^{RMS} = 5.6 \pm 1.0$  fm, the delay between the emission of the neutrons  $\tau_{nn}$  needed to describe the n-n correlation function for the C target may be introduced. As discussed above, this delay should correspond to the lifetime of the resonances. The result of a  $\chi^2$  analysis, represented by the dashed lines in Fig. 3 (bottom right panel), suggests an average lifetime of  $150_{-150}^{+250}$  fm/c.

---

\*) The present data are not particularly sensitive to the location and form of the states, in particular below 1 MeV, and a level at 0.5 MeV would, for example, equally well describe the data.

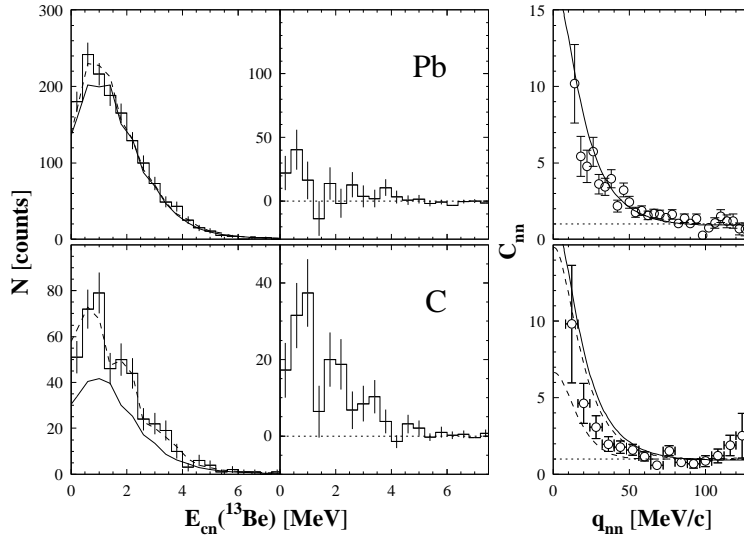


Fig. 3. Core-n relative energy distributions (left) and n-n correlation functions (rightmost panels) for the dissociation of  $^{14}\text{Be}$  by Pb and C. The lines in the  $E_{cn}$  spectra are the result of the phase-space model simulations with n-n FSI (solid) plus core-n FSI (dashed, see text). The histograms presented in the middle panels are the difference between the data and the n-n FSI simulations. The solid lines in the panels at the right are the  $C_{nn}$  for  $r_{nn}^{RMS} = 5.6$  fm and  $\tau_{nn} = 0$ ; the dashed lines correspond to the limits of the range  $r_{nn}^{RMS} = 6.6\text{--}4.6$  fm and  $\tau_{nn} = 0\text{--}400$  fm/c.

#### §4. Multineutron Clusters

The very lightest nuclei have long played a fundamental role in testing nuclear models and the underlying nucleon-nucleon interaction. In this context the study of systems exhibiting very asymmetric  $N/Z$  ratios may provide new perspectives on the nucleon-nucleon interaction and few-body forces. In the case of the light, two-neutron halo nuclei such as  $^6\text{He}$ , insight is already being gained into the effects of the three-body force<sup>17)</sup>. Very recently evidence has been presented that the ground state of  $^5\text{H}$  exists as a relatively narrow, low-lying resonance<sup>18)</sup>. In the case of the lightest  $N = 4$  isotone,  $^4\text{n}$ , nothing is known<sup>19), 20)</sup>. The discovery of such neutral systems as bound states would have far reaching implications for many facets of nuclear physics.

It is, therefore, interesting to speculate that multineutron halo nuclei and other very neutron-rich systems may contain components of the wavefunction in which the neutrons present a relatively compact cluster-like configuration. If this were to be the case, then the dissociation of beams of such nuclei may offer a means to produce bound neutron clusters (if they exist) and, more generally study multineutron correlations.

To date the majority of searches for multineutron systems have relied on very low (typically  $\sim 1$  nb) cross section double-pion charge exchange ( $D\pi\text{CX}$ ) and heavy-ion transfer reactions (see, for example, refs<sup>16), 21)</sup>). In the case of dissociation of an energetic beam of a very neutron-rich nucleus, relatively high cross sections (typically

$\sim 100$  mb) are encountered. Thus, even only a small component of the wavefunction corresponding to a multineutron cluster could result in a measurable yield with a moderate secondary beam intensity. Furthermore the backgrounds arising in  $D\pi CX$  and heavy-ion transfer reactions from target impurities and complex many-body phase space reactions are obviated in breakup.

The difficulty in this approach lies in the direct detection of a  $^A n$  cluster. The avenue that we have explored is to detect the recoiling proton in a liquid scintillator<sup>22)</sup>. One of the principle advantages of a liquid scintillator is that neutrons may be discriminated with good efficiency from the  $\gamma$  and cosmic-ray backgrounds using pulse-shape analysis. Careful source and cosmic-ray calibrations<sup>\*)</sup> permit the charge deposited and hence the energy ( $E_p$ ) of the recoiling proton to be determined. This may be compared to the energy derived from the measured time-of-flight ( $E_n$ ): for a single neutron and an ideal detector,  $E_p/E_n \leq 1$ ; for a realistic detector with finite resolution the limit is  $\sim 1.4$ . In the case of a multineutron cluster ( $^A n$ )  $E_p$  can exceed the incident energy per nucleon and  $E_p/E_n$  will take on a range of values extending beyond 1.4 — up to  $\sim 3$  in the case of  $A=4$  (Fig. 4).

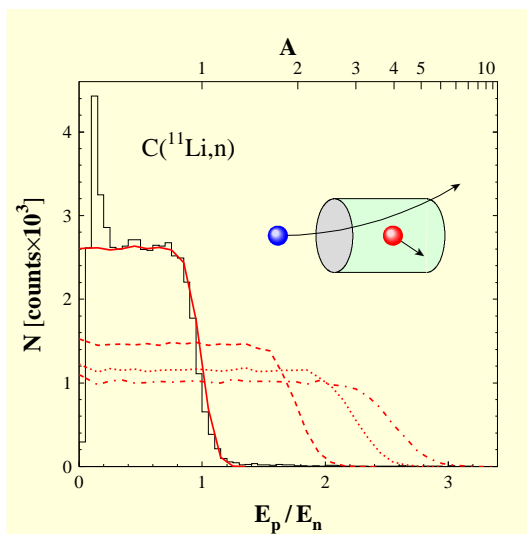


Fig. 4.  $E_p/E_n$  for  $A=1$  (solid line), 2 (dashed), 3 (dotted) and 4 (dot-dashed). In the case of  $A=1$ , comparison is made to single neutron events from the  $^{11}\text{Li}$  breakup of  $^{11}\text{Li}$ . The excess of events at low  $E_p/E_n$  arise from reactions on the carbon component of the scintillator.

As discussed in ref.<sup>22)</sup>, the DEMON modules exhibit saturation effects at very high light output<sup>\*\*)</sup>. In order to avoid this problem, particularly in the region  $E_p/E_n < 1$ , an upper limit of  $E_n = 18$  MeV/nucleon was imposed.

\*) The astute reader will also realise that the maximum proton recoil energy for a given  $E_n$  may also be used for calibration purposes — a procedure that we are currently employing.

\*\*\*) The initial goal of the experiment run to acquire the data analysed here was not the search for multineutron clusters, and as such the analysis of very high light outputs was not foreseen. The possibility of operating the DEMON photomultipliers at lower voltages is being explored for future dedicated experiments.

At low energies the proton recoil is free of saturation effects. However, background events arising from  $\gamma$  and cosmic rays represent a potential contaminant for the  $E_p/E_n$  distribution. These events are randomly distributed in time, and thus the relative rate increases at low energy since  $E \propto t^{-2}$ . As the energy loss in a module is completely uncorrelated with the inferred time-of-flight,  $E_p/E_n$  is not confined to values inferior to 1.4. Even if the rejection rate using pulse-shape analysis is close to 100 %, any events that remain could mimic a  ${}^A\text{n}$  signal. As detailed in ref. <sup>22)</sup>, a lower limit on  $E_n$  of 11 MeV/nucleon was thus imposed. Importantly, any such events which do survive these conditions should not be correlated with any particular breakup fragment.

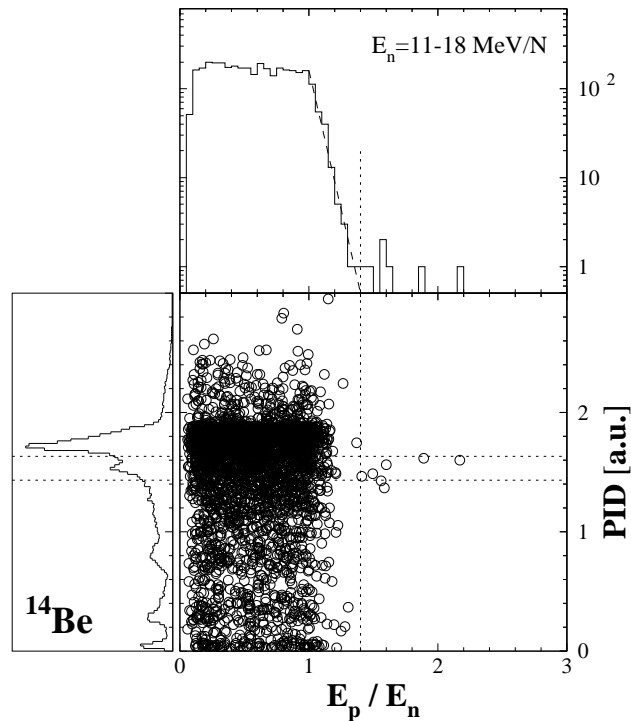


Fig. 5. PID versus  $E_p/E_n$  for the reaction ( ${}^{14}\text{Be}, X+n$ ). The prominent peak at  $\text{PID} \sim 1.7$  corresponds to  ${}^{12}\text{Be}$  fragments. The horizontal band (dotted line) corresponds to the range of PID values encompassing the  ${}^{10}\text{Be}$  fragments.

The data already at hand from the study of the dissociation of  ${}^{14}\text{Be}$  and  ${}^{11}\text{Li}$  <sup>3) - 5)</sup> was examined with a view to testing the method outlined above. The details of the analyses carried out may be found in ref. <sup>22)</sup>. The essential results are provided by figures 5 and 6 which display the charged fragment particle identification (PID) derived from the Si-CsI detector telescope versus  $E_p/E_n$ .

The  $E_p/E_n$  distributions (upper panels in Figs. 5 and 6) exhibit a general trend below 1.4: a plateau up to 1 followed by a sharp decline, which may be fitted to an exponential distribution (dashed line). In the region where  ${}^A\text{n}$  events may be expected to appear some 7 events with  $E_p/E_n$  ranging from 1.4 to 2.2 are observed for



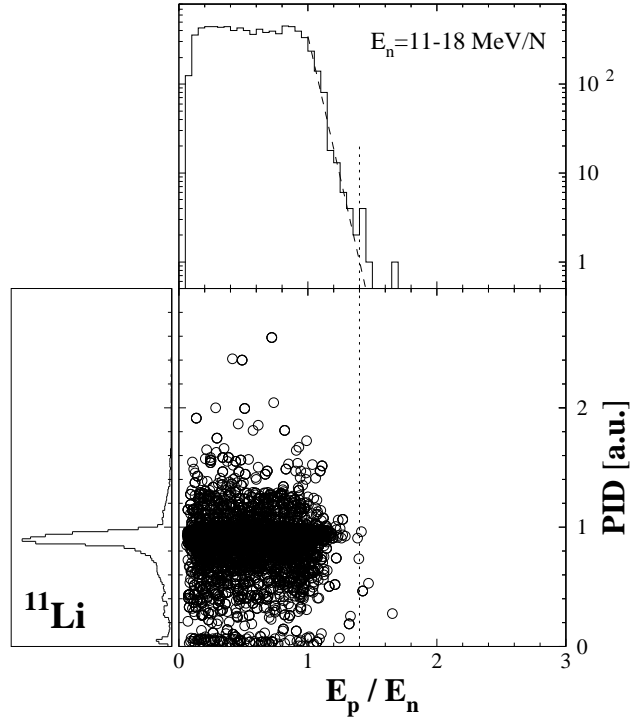


Fig. 6. PID versus  $E_p/E_n$  for the breakup of  $^{11}\text{Li}$ . The prominent peak at  $\text{PID} \sim 9$  corresponds to  $^9\text{Li}$  fragments.

$^{14}\text{Be}$ . In the case of  $^{11}\text{Li}$ , despite the greater number of neutrons detected (factor of 2.4), only 4 events appear which lie just above threshold. Turning to the coincidences with the charged fragments, the 7 events produced by the  $^{14}\text{Be}$  beam fall within a region centred on  $^{10}\text{Be}$ . In the case of the 4 events produced in the reactions with  $^{11}\text{Li}$  no correlation appears to exist with any particular fragment.

The left panel in figure 7 displays in more detail the region of the particle identification spectrum for the breakup of  $^{14}\text{Be}$  into lighter Be isotopes, together with the 7 events in question. Clearly the resolution in PID does not allow the observed events to be unambiguously associated with a  $^{10}\text{Be}$  fragment. However, the much higher cross-section for this channel ( $460 \pm 40 \text{ mb}$ ) compared to  $^{11}\text{Be}$  ( $145 \pm 20 \text{ mb}$ ) suggests that this may be the case. It should be noted that the PID is somewhat complicated by the fact that reactions also occur in the Si-CsI telescope. The effects of this are shown in figure 7 (right panel), whereby the reactions in the telescope give rise to a tail extending to higher mass Be fragments. Ideally a dedicated experiment including a high statistics target-out measurement would remove this ambiguity.

As a first step towards investigating the nature of the events with  $E_p/E_n < 1.4$  each was examined to verify that it corresponded to a well defined event in both the charged particle and neutron detectors. Of the 7 events observed in the breakup of  $^{14}\text{Be}$ , all but one survived. The 6 remaining events thus appear to exhibit characteristics consistent with detection of a multineutron cluster from the breakup of  $^{14}\text{Be}$ .

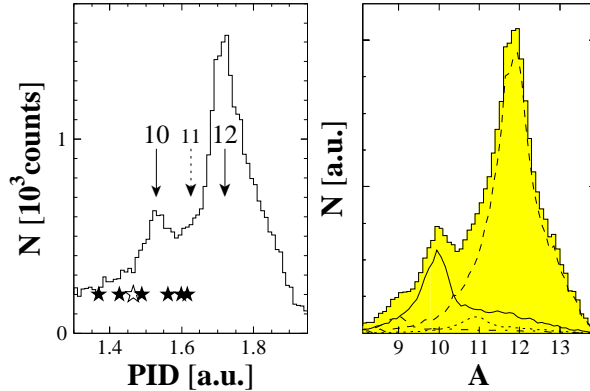


Fig. 7. Left: detail of the particle identification spectrum around  $^{10,12}\text{Be}$  for the data from the reaction ( $^{14}\text{Be}, \text{X}+\text{n}$ ); the 7 events with  $E_p/E_n > 1.4$  are denoted by the symbols. Right: results of a simulation of the reactions ( $^{14}\text{Be}, ^{9-12}\text{Be}$ ) in the target and telescope; the shaded histogram is the sum of the contributions from all four fragments.

Potential sources of such events not involving the formation of a multineutron were consequently examined<sup>22)</sup>.

Table I. Comparison of the number of events observed (exp) with  $E_p/E_n > 1.4$  for each channel with the estimated number of events expected from pile-up. The methods are based on a Monte-Carlo simulation (sim), and the relative-angle distribution of n-n pairs (nn). The latter is quoted in terms of a conservative upper limit<sup>22)</sup>.

Channel	$N_{2n}^{\text{exp}}$	$N_{2n}^{(\text{sim})}$	$N_{2n}^{(\text{nn})}$
( $^{11}\text{Li}, \text{X}$ )	4	$\sim 3$	$< 7.0$
( $^{14}\text{Be}, ^{12}\text{Be}$ )	0	0.8	$< 1.2$
( $^{14}\text{Be}, ^{10}\text{Be}$ )	6	0.2	$< 0.8$

The most obvious source of events that may mimic a multineutron cluster is the detection, in the same event, of more than one neutron in the same module. The rates at which such pile-up is expected to occur have been examined in detail employing both simulations which reproduce the observed neutron angular, energy and multiplicity distributions, together with an analysis based on the measured neutron-neutron relative angle distributions<sup>22)</sup>. As summarised in Table I, the two methods provide consistent results which are in line with the numbers of events observed for the channels ( $^{11}\text{Li}, \text{X}+\text{n}$ ) and ( $^{14}\text{Be}, ^{12}\text{Be}+\text{n}$ ). In the case of ( $^{14}\text{Be}, ^{10}\text{Be}$ ), less than one event arising from pile-up is estimated to occur with  $E_p/E_n < 1.4$ , compared to some 6 observed events. Given such results we conclude that reasonable evidence exists for the production of a multineutron cluster in the breakup of  $^{14}\text{Be}$  — most probably in the channel  $^{10}\text{Be}+4\text{n}$ .

The average flight time of the 6 events from the target to DEMON is  $\sim 100$  ns. This indicates that the lifetime must be of this order or longer. The conditions applied in the analysis make an estimate of the production cross-section rather difficult.

Nonetheless, if we assume that these conditions affect the number of neutrons and  ${}^4\text{n}$  in a similar manner, we can scale the cross-section measured for the production of  ${}^{10}\text{Be}^{3)}$  by the relative yield observed and obtain  $\sigma({}^4\text{n}) \sim 1$  mb.

## §5. Conclusions

An experimental programme to explore clustering and correlations in halo systems has been described. New approaches have been developed, including the application of neutron-neutron interferometry and Dalitz-plot analyses to the dissociation of two-neutron halo nuclei. Attempts to produce and detect directly bound multi-neutron clusters have also been described and the results from a measurement of the breakup of  ${}^{14}\text{Be}$  discussed.

Very recently a high statistics measurement of the dissociation of  ${}^6\text{He}$  has been carried out. Given that  ${}^6\text{He}$  is structurally the most well known two-neutron halo system, this work should provide a good test of the techniques described here to probe correlations. Furthermore, correlation function analyses employing the longitudinal and transverse neutron-neutron relative momenta should provide an independent means to disentangle the halo neutron-neutron separation and time delay in emission. Measurements in the coming year with a  ${}^8\text{He}$  beam should allow multineutron correlations to be explored.

In terms of neutron clusters the confirmation or otherwise of the events observed here with a higher intensity  ${}^{14}\text{Be}$  beam and improved fragment detection system is planned for the coming year. The search for similar events in the breakup of  ${}^8\text{He}$  will also be undertaken. The saturation effects encountered with DEMON at high light outputs will be reduced by lowering the beam energy (in the case of the  ${}^8\text{He}$  measurement) as well as the high voltage applied to the photomultipliers. In the longer term, searches for heavier multineutron clusters could be envisaged when more neutron-rich beams become available at intensities beyond  $10^2$  pps.

## §6. References

### Acknowledgements

I would like to draw special attention to the key rôles played by Miguel Marqués (correlations and neutron clusters) and Marc Labiche ( ${}^{14}\text{Be}$  breakup) in the work described here. It is also a pleasure to thank the members of the E295 collaboration and, in particular, the DEMON and CHARISSA crews for their contributions. The support provided by the staffs of LPC (in particular JM Gautier, P Desrues, JM Fontbonne, L Hay, D Etasse, J Tillier) and GANIL (R Hue, C Cauvin, R Alves Conde) in preparing and executing the experiments is gratefully acknowledged.

This work was funded under the auspices of the IN2P3-CNRS (France) and EPSRC (United Kingdom). Additional support from the ALLIANCE programme (Ministère des Affaires Etrangères and British Council) and the Human Capital and Mobility Programme of the European Community (Access to Large Scale Facilities) is also acknowledged.

## References

- 1) M. Freer *et al.*, Phys. Rev. Lett. **82** (1999) 1383;  
M. Freer *et al.*, Phys. Rev. **C63** (2001) 034301 and refs therein
- 2) F.M. Marqués *et al.*, Nucl. Inst. Meth. **A450** (2000) 109
- 3) M. Labiche *et al.*, Phys. Rev. Lett. **86** (2001) 600;  
M Labiche, Thèse, Université de Caen, (1999), LPCC T 99-03
- 4) F.M. Marqués *et al.*, Phys. Lett. **B476** (2000) 219
- 5) F.M. Marqués *et al.*, Phys. Rev. **C64** (2001) 061301R
- 6) R. Hanbury-Brown, R. Twiss, Philos. Mag. **45** (1954) 663
- 7) G. Goldhaber *et al.*, Phys. Rev. **120** (1960) 300
- 8) D.H. Boal *et al.*, Rev. Mod. Phys. **62** (1990) 553
- 9) R. Lednicky, L. Lyuboshits, Sov. J. Nucl. Phys. **35** (1982) 770
- 10) E. Sauvan *et al.*, Phys. Rev. Lett. **87** (2001) 042501
- 11) R.H. Dalitz, Philos. Mag. **44** (1953) 1068
- 12) A.N. Ostrowski *et al.*, Z. Phys. **A343** (1992) 489
- 13) A.V. Belozorov *et al.*, Nucl. Phys. **A636** 419 (1998) 419
- 14) K.L. Jones, Thesis, University of Surrey (2000);  
N.A. Orr, in Proc. of the Tours Symposium on Nuclear Physics, AIP Conf. Proceedings (2001) nucl-ex/0011002 and refs therein
- 15) M. Thoennessen *et al.*, Phys. Rev. **C63** 014308 (2001) 014308
- 16) J. Grüter *et al.*, Eur. Phys. J. **4** (1999) 5
- 17) M.V. Zhukov *et al.*, Phys. Rep. **231**, 151 (1993) 151
- 18) A.A. Korshennikov *et al.*, Phys. Rev. Lett. **87** (2001) 092501
- 19) D.R. Tilley, H.R. Weller, G.M. Hale, Nucl. Phys. **A541** (1992) 1 and references therein
- 20) A.A. Ogloblin, Y.E. Penionzhkevich, in *Treatise on Heavy-Ion Science (vol. 8): Nuclei Far From Stability*, ed. D.A. Bromley (Plenum Press, New York, 1989) p 261 and references therein
- 21) H.G. Bohlen *et al.*, Nucl. Phys. **A583** (1995) 775
- 22) F.M. Marqués *et al.*, nucl-ex/0111001